Mem. S.A.It. Vol. 81, 1095

Memorie della

Low–metallicity AGB models: the H profile in the ^{13}C-pocket and the effect on the *s*-process

S. Bisterzo[1] and S. Cristallo[2,3]

[1] Dipartimento di Fisica Generale, Università di Torino, 10125 (To) Italy
e-mail: bisterzo@ph.unito.it
[2] Departamento de Fisica Teorica y del Cosmos, Universidad de Granada, Campus de Fuentenueva, 18071 Granada, Spain
[3] INAF Osservatorio Astronomico di Collurania, via M. Maggini, 64100 Teramo, Italy

Abstract. The ^{13}C(α, n)^{16}O reaction is the major neutron source in low-mass asymptotic giant branch (AGB) stars, where the main and the strong *s*-process components are synthesised. After a third dredge-up (TDU) episode, ^{13}C burns radiatively, in a thin pocket which forms in the top layers of the He-intershell, by proton capture on the abundant ^{12}C. Therefore, mixing of a few protons from the H-rich envelope into the He-rich region is required. However, the origin and the efficiency of this mixing episode are still matters for debate and, consequently, the formation of the ^{13}C-pocket represents a significant source of uncertainty that affects AGB models. We analyse the effects on the nucleosynthesis of the s-elements caused by the variation of the hydrogen profile in the region where the ^{13}C-pocket forms for an AGB model with $M = 2\,M_\odot$ and [Fe/H] = -2.3. In particular, we concentrate on three isotopes (^{89}Y, ^{139}La and ^{208}Pb), chosen as representative of the three *s*-process peaks.

Key words. Stars: C and s rich – Stars: abundances – Stars: nucleosynthesis

1. Introduction

During their thermally pulsing (TP) phase, low-mass asymptotic giant branch (AGB) stars are the site of the main and the strong component of the *s*-process, which is responsible for the nucleosynthesis of half the nuclei from Sr to Pb/Bi. After a limited number of pulses, the convective envelope penetrates into the He-intershell at the quenching of each convective instability, mixing freshly synthesized ^{4}He, ^{12}C and *s*-process elements to the surface (third dredge-up, TDU).

The major neutron source in low-mass AGB stars is the ^{13}C(α,n)^{16}O reaction, which burns radiatively during the interpulse period in a thin region at the top of the He-intershell (^{13}C-pocket). The physical mechanism that allows the formation of the ^{13}C-pocket is debated. A small number of protons are assumed to penetrate from the envelope into the He-intershell during TDU episodes (Iben & Renzini 1982). Then, at H reignition, a large amount of ^{13}C is synthesised in the top layers of the intershell by the ^{12}C(p,γ)^{13}N($\beta^{+}\nu$)^{13}C nuclear chain. This ^{13}C is of primary origin and, therefore, independent of the metallicity. During the interpulse, the H-burning shell ad-

Send offprint requests to: P. Bonifacio

vances in mass, compressing and heating the underlying material, and at $T \approx 0.9 \times 10^8$ K the $^{13}C(\alpha,n)^{16}O$ reaction starts releasing neutrons in radiative conditions. Later on, the synthesised *s*-process nuclei are engulfed and diluted in the next convective region generated by TP.

Different evolutionary and post-processing codes have been developed in recent years to understand nucleosynthesis in low-mass AGB stars (e.g. Straniero et al. 1995, 2003; Gallino et al. 1998; Goriely & Mowlavi 2000; Karakas & Lattanzio 2003, 2007; Campbell & Lattanzio 2008; Straniero et al. 2006). Several mechanisms have been proposed to reproduce the mixing leading to the ^{13}C-pocket formation. These include semi-convection, models with rotation (Langer et al. 1999; Herwig et al. 2003; Siess et al. 2004), gravity waves (Denissenkov & Tout 2003), exponential diffusive overshooting at the borders of all convective zones (Herwig et al. 1997) and opacity-induced overshooting at the base of the convective envelope (Straniero et al. 2006). A clear answer to the properties of such mixing has not been reached yet.

We test here the effects on the nucleosynthesis of the *s* elements by adopting different H profiles in the region of the ^{13}C-pocket forming after the first TDU of an AGB model with initially $M = 2\,M_\odot$ and [Fe/H] = −2.3. Comparison between the full evolutionary FRANEC (Frascati Raphson-Newton Evolutionary Code) models (Cristallo et al. 2009, hereinafter C09) and FRANEC models coupled with a post-processing nucleosynthesis method (Gallino et al. 1998; Bisterzo et al. 2010) are presented.

2. Results

C09 introduce a mixing algorithm which depends on a free parameter[1] in their full evolutionary models to mimic the formation of a transition zone between the fully convective envelope and the radiatively stable H-exhausted core. Thus, a partial mixing of protons takes place and leads to the formation of a ^{13}C rich layer. Its mass and profile decrease with the number of pulses (see C09, their figs 4 and 8).

Fig. 1, top panel, shows this region. In the uppermost layers of the pocket, where protons are more abundant, the ^{13}C-pocket overlaps with a ^{14}N-pocket, which forms via the $^{13}C(p,\gamma)^{14}N$ reaction. ^{14}N acts as a neutron poison via the resonant reaction $^{14}N(n,p)^{14}C$. Thus by subtracting neutrons from the nucleosynthesis of the *s*-process elements. Fig. 1, bottom panel, shows the same mass region at the end of the ^{13}C burning. We concentrate on three isotopes, ^{89}Y, ^{139}La and ^{208}Pb, chosen as representative of the three *s*-process peaks. As expected, at this low metallicity, a large amount of ^{208}Pb is produced (Gallino et al. 1998). Maximum Pb production occurs in the central layers of the pocket where $X(^{13}C) > X(^{14}N)$ (we find $X(^{208}Pb) = 4.5 \times 10^{-5}$), while Y and La show definitely lower abundances: $X(^{89}Y) \approx X(^{139}La) \approx 6 \times 10^{-9}$. In the outer and inner regions of the pocket, however, ^{89}Y and ^{139}La show peaked distributions. Note that, in the outer tail, *s*-process elements are efficiently synthesised even if $X(^{13}C) < X(^{14}N)$.

In order to test the effect of these tails on Y, La and Pb with different H profiles, we use the post-processing nucleosynthesis models described by Bisterzo et al. (2010). We adopt the H profile of Gallino et al. (1998, case ST, their fig. 2). Then we introduce a further region in the pocket (with mass $M = 4 \times 10^{-4}\,M_\odot$) in which we change the abundances of ^{13}C and ^{14}N to simulate different H profiles in the tails. We multiply or divide by different factors the ^{13}C and ^{14}N abundances in the pocket[2]. Note that the H profile and the mass of the pocket are kept constant pulse by pulse. The envelope abundances of the two *s*-process indices [La/Y] and [Pb/La] obtained with the post-processing method are shown in Tables 1 and 2. In Table 1, first group, we show the results computed with standard ^{13}C-pockets (with three zones as Gallino et al. 1998) for various ^{13}C-pocket efficiencies (from

[1] See C09 for the procedure followed to calibrate it.

[2] In fact a range of ^{13}C-pockets is introduced in order to interpret the spread in the *s*-elements observed in CEMP-*s* stars.

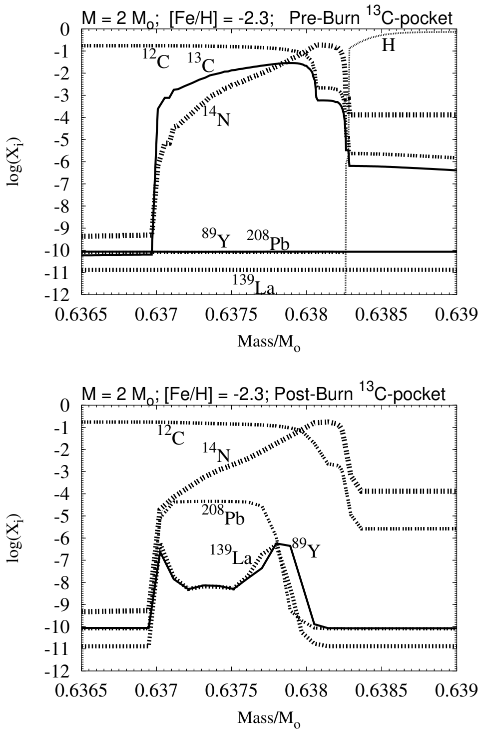

Fig. 1. ^{13}C-pocket mass region for a full evolutionary AGB model of $M = 2\,M_\odot$ and [Fe/H] $= -2.3$ (C09) after the first TDU, at the pocket formation (*top panel*) and at the end of the ^{13}C burning (*bottom panel*).

ST $\times$ 2 down to ST/24). These results are compared with models with an added fourth zone with $X(^{13}\mathrm{C}) < X(^{14}\mathrm{N})$ (Table 1, second group). This has been done to simulate the effect induced by the outer tail of the pocket shown in Fig. 1 by C09 model on post-processing calculation results. C09 obtain a final [La/Y] = 0.45 and [Pb/La] = 1.30. With the post-processing method and a range of standard ^{13}C-pockets, [La/Y] reaches a maximum value of about 0.9 (case ST/6) and [Pb/La] $\approx$ 2.2 (case ST/1.5). When adding the fourth zone, minimal variations are found for large and low ^{13}C-pocket efficiencies, while appreciable differences are found in the intermediate cases. For large ^{13}C abundances (case ST$\times$2), the addition of fourth zone leads to a large production of light elements (Ne, Na and Mg) whose poisoning effect induces a slightly decrease in the final *s*-process element surface overabundances. For very low ^{13}C efficiencies the *s*-process production is mainly due to the ^{22}Ne(α, n)^{25}Mg reaction (Bisterzo et al. 2010). This minimizes the effects of additional ^{13}C and^{14}N. For intermediate cases the introduction of the fourth zone instead reduces the maximum [La/Y] to about 0.5 dex and the maximum [Pb/La] to about 1.6,dex. In Table 2 we select the highest ^{13}C-pocket case (case ST $\times$ 2) and we test the effect of an added fourth zone with different $X(^{13}\mathrm{C})$ values (assuming $X(^{14}\mathrm{N})$ is negligible). We choose the ST $\times$ 2 case because previous comparisons done at larger metallicities (C09) indicate that the best agreement between post-processed and full evolutionary models is found with this case. The standard case with three zones only (column II) gives [La/Y] = 0.50 and [Pb/La] = 2.04, while the addition of a fourth zone with $X(^{13}\mathrm{C}) = 3.8 \times 10^{-4}$ (test III) definitely lowers the [Pb/La] ratio (to 1.47) leaving practically untouched the [La/Y] ratio (at 0.56). Thus, a reasonable agreement between this test and C09 is found even at such low metallicities. After verifying that the tails of the ^{13}C-pocket affect the *s* distribution, one may constrain the choice of the H profile through a study of spectroscopic observations in CEMP-*s* stars. Note that, for disc metallicities, the tails of the pocket do not influence the *s* distribution noticeably.

3. Conclusions

The maximum amount of ^{13}C and ^{14}N in the pocket and different hydrogen profiles (and therefore the amount of ^{13}C and ^{14}N in the tails of the pocket) modify the *s* abundance distribution. In particular, the *s*-process indices [La/Y] and [Pb/La] are sensitive to the tails of the pocket. At [Fe/H] $= -2.3$ a large amount of ^{208}Pb is produced when $X(^{13}\mathrm{C}) > X(^{14}\mathrm{N})$. A first interesting consequence caused by the addition of an outer tail in the pocket with $X(^{13}\mathrm{C}) < X(^{14}\mathrm{N})$ is that the maximum [La/Y] value attained with different ^{13}C-efficiencies is reduced to about 0.5. Moreover, with a calibrated extra $X(^{13}\mathrm{C})$ in the tails of the pocket, the maximum [Pb/La] is reduced to 1.4 dex. Comparison between theory and observations

Table 1. Envelope abundances of [Y/Fe], [La/Fe], [Pb/Fe] and their ratios, [La/Y] and [Pb/La], for a post-processing model of $M = 2\,M_\odot$ and [Fe/H] = −2.3 and various ^{13}C-pocket efficiencies (from ST × 2 down to ST/24). The first group lists the results obtained with the standard ^{13}C-pocket, while in the second group a further fourth zone with $X(^{13}\mathrm{C}) < X(^{14}\mathrm{N})$ is added.

Cases		ST × 2	ST	ST/1.5	ST/2	ST/6	ST/12	ST/24
	[Y/Fe]	1.68	1.39	1.33	1.35	1.98	2.35	2.45
	[La/Fe]	2.18	1.88	1.92	2.10	2.85	2.94	2.71
	[Pb/Fe]	4.22	4.12	4.09	4.06	3.82	3.44	2.69
	[La/Y]	0.50	0.49	0.59	0.75	0.87	0.59	0.26
	[Pb/La]	2.04	2.24	2.17	1.96	0.97	0.50	-0.02
	$X(^{13}\mathrm{C})$=	7.2E-2	3.7E-2	2.5E-2	1.9E-2	6.2E-3	3.1E-3	1.6E-3
	$X(^{14}\mathrm{N})$=	2.7E-1	1.4E-1	9.3E-2	7.1E-2	2.3E-2	1.2E-2	5.8E-3
zone 4	[Y/Fe]	1.58	1.75	1.89	2.00	2.40	2.58	2.64
$X(^{13}\mathrm{C}) < X(^{14}\mathrm{N})$	[La/Fe]	2.10	2.25	2.42	2.54	2.92	2.97	2.80
	[Pb/Fe]	4.04	4.02	3.99	3.97	3.76	3.43	2.84
	[La/Y]	0.52	0.50	0.53	0.54	0.52	0.39	0.16
	[Pb/La]	1.94	1.77	1.57	1.43	0.84	0.46	0.04

Table 2. The same as Table 1, but for a case ST × 2 and an added fourth zone with different $X(^{13}\mathrm{C})$ values, from 0 (standard case) up to 4.3×10^{-3}. $X(^{14}\mathrm{N})$ is assumed to be negligible. In the last column the results obtained by C09 are listed.

zone 4,	standard	I test	II test	III test	IV test	V test	VI test	VII test	C09
$X(^{13}\mathrm{C})$	0.0	2.9E-4	3.5E-4	3.8E-4	4.8E-4	5.8E-4	1.2E-3	4.3E-3	
[Y/Fe]	1.68	2.23	2.21	2.19	2.09	1.97	1.74	1.75	1.12
[La/Fe]	2.18	2.60	2.65	2.75	2.80	2.76	2.48	2.27	1.57
[Pb/Fe]	4.22	4.21	4.23	4.22	4.23	4.24	4.29	4.33	2.88
[La/Y]	0.50	0.37	0.44	0.56	0.71	0.79	0.74	0.52	0.45
[Pb/La]	2.04	1.61	1.58	1.47	1.43	1.48	1.81	2.06	1.30

in CEMP-*s* stars is then needed in order to constrain the choice of the H profile in the central and outer regions of the ^{13}C-pocket during AGB nucleosynthesis.

Acknowledgements. We are grateful to Roberto Gallino for helpful comments and discussions.

References

Bisterzo, S., Gallino, R., Straniero, O., Cristallo, S., Käppeler, F. 2010, MNRAS, 404, 1529

Campbell, S. W., & Lattanzio, J. C. 2008, A&A, 490, 769

Cristallo, S., Straniero, O., Gallino, R., et al. 2009, ApJ, 696, 797 [C09]

Denissenkov, P. A., & Tout, C. A. 2003, MNRAS, 340, 722

Gallino, R., Arlandini, C., Busso, M., et al. 1998, ApJ, 497, 388

Goriely, S., & Mowlavi, N. 2000, A&A, 362, 599

Herwig, F., Blöcker, T., Schönberner, D., El Eid, M. 1997, A&A, 324, L81

Herwig, F., Langer, N., Lugaro, M. 2003, ApJ, 593, 1056

Karakas, A., & Lattanzio, J. 2003, PASA, 20, 279

Karakas, A., & Lattanzio, J. 2007, PASA, 24, 103
Iben, I. Jr., & Renzini, A. 1982, ApJ, 259, L79
Langer, N., Heger, A., Wellstein, S., Herwig, F. 1999, A&A, 346, L37
Siess, L., Goriely, S., & Langer, N. 2004, A&A, 415, 1089
Straniero, O., Gallino, R., Busso, M., et al. 1995, ApJ, 440, 85
Straniero, O., Domínguez, I., Cristallo, S., Gallino, R. 2003, PASA, 20, 389.
Straniero, O., Gallino, R, & Cristallo, S. 2006, Nucl. Phys. A, 777, 311